

**Characteristics of
Monsoon inversions
over Arabian Sea**

Sanjeev Dwivedi et al.

This discussion paper is/has been under review for the journal Atmospheric Chemistry and Physics (ACP). Please refer to the corresponding final paper in ACP if available.

Characteristics of Monsoon inversions over Arabian Sea observed by satellite sounder and reanalysis data sets

Sanjeev Dwivedi¹, M. S. Narayanan¹, M. Venkat Ratnam², and D. Narayana Rao¹

¹Department of Physics, SRM University, Kattankulathur, Chennai, 603 203, India

²National Atmospheric Research Laboratory (NARL), Gadanki, Tirupati, 517 502, India

Received: 14 September 2015 – Accepted: 3 December 2015 – Published: 15 December 2015

Correspondence to: M. Venkat Ratnam (vratnam@narl.gov.in)

Published by Copernicus Publications on behalf of the European Geosciences Union.

Title Page

Abstract

Introduction

Conclusions

References

Tables

Figures



Back

Close

Full Screen / Esc

Printer-friendly Version

Interactive Discussion



Abstract

Monsoon inversions (MIs) over Arabian Sea (AS) are an important characteristic associated with the monsoon activity over Indian region during summer monsoon season. In the present study, we have used five years (2009–2013) data of temperature and water vapor profiles obtained from satellite sounder instrument, Infrared Atmospheric Sounding Interferometer (IASI) onboard MetOp satellite, besides ERA-Interim data, to study their characteristics. The lower atmospheric data over the AS have been examined first to identify the areas where monsoon inversions are predominant and occur with higher strength. Based on this information, a detailed study has been made to investigate their characteristics separately in eastern AS (EAS) and western AS (WAS) to examine their contrasting features. The initiation and dissipation times of MI, their percentage occurrence, strength etc., has been examined using the huge data base. The relation with monsoon activity (rainfall) over Indian region during normal and poor monsoon years is also studied. WAS ΔT values are ~ 2 K less than those over the EAS, ΔT being temperature difference between 950 and 850 hPa. A much larger contrast between WAS and EAS in ΔT is noticed in ERA-Interim dataset. Vis a Vis those observed by satellites. The possibility of detecting MI from another parameter, Refractivity N , obtained directly from another satellite constellation of GPS RO (COSMIC), has also been examined. MI detected from IASI and Atmospheric InfraRed Sounder (AIRS) sounder onboard NOAA satellite have been compared to see how far the two data sets can be combined to study the MI characteristics. We suggest MI could also be included as one of the semi-permanent features of southwest monsoon along with the presently accepted six parameters.

1 Introduction

The Monsoon Inversion (MI) is one of the criteria providing a stability condition over the western Arabian Sea (AS), extending sometimes through to the west coast of India.

ACPD

15, 35277–35312, 2015

Characteristics of Monsoon inversions over Arabian Sea

Sanjeev Dwivedi et al.

Title Page

Abstract

Introduction

Conclusions

References

Tables

Figures



Back

Close

Full Screen / Esc

Printer-friendly Version

Interactive Discussion



Characteristics of Monsoon inversions over Arabian Sea

Sanjeev Dwivedi et al.

Title Page

Abstract

Introduction

Conclusions

References

Tables

Figures



Back

Close

Full Screen / Esc

Printer-friendly Version

Interactive Discussion



The MI controls the mid tropospheric moisture content during the different phases of the monsoon. This shallow layer of low level inversion will act as a barrier in uplifting of the moisture, and could act like a wave – guide for transport of water vapour to the mainland. The fluctuation of the rainfall over the west coast of India is more closely related to changes in monsoon circulation over the AS (Das, 2002). Thus, MI has been known to be intimately associated with the activity of the Indian southwest monsoon and have a close link with active and break spells (Narayanan and Rao, 2004).

MI's were first detected in 1964 during International Indian Ocean Expedition (IIOE) from ship radiosonde data by Colon (1964) and Ramage (1966). Subsequently from satellite derived temperature and humidity data, this feature was detected by Narayanan and Rao (1981). They detected MI despite the coarse vertical resolution (~ 2 km) of the TIROS-N satellite temperature sounding instruments (Thomas, 1980) of 1970–1980's compared to the vertical extent (about 1 to 1.5 km) of the phenomena itself. They used a simple differencing technique by finding the difference, ΔT , of sea skin temperature and 1000 to 850 hPa mean layer temperature (MLT) from the satellite sounding data. By adopting this differencing procedure, they assumed that most of the systematic errors/limitations of retrieval methods and vertical resolution of satellite soundings may be getting significantly minimized. Furthermore, the spatial and temporal nature of MI's is quite large compared to normal boundary layer inversions observed over land and other oceans.

Using data of about 150 ship radiosonde and aircraft dropsonde profiles and concurrent TIROS-N satellite sounder data of MONsoonEXperiment (MONEX) conducted in 1979, they showed that regions with $\Delta T \leq 2$ K in satellite derived atmospheric temperatures are associated with AS MI. Study of these MI's over the western AS was one of the three major objectives of MONEX/FGGE-1979 (WMO, 1976). These are seen to be much stronger (temperature departures from normal profiles in some cases being as high as ~ 6 K in the lower 1–2 km height region) in contrast to the inversions observed over land or associated with trade wind inversions (~ 1 –2 K).

Characteristics of Monsoon inversions over Arabian Sea

Sanjeev Dwivedi et al.

Title Page

Abstract

Introduction

Conclusions

References

Tables

Figures



Back

Close

Full Screen / Esc

Printer-friendly Version

Interactive Discussion



5 MIs are characterized by both a vertical temperature increase in the altitude region from 0.5 km (in some cases even from surface) to ~ 2 km and with a sharp fall in relative humidity (RH) above this altitude region. Some of the observed features of MIs reported from the limited observations to date (Colon, 1964; Ramage, 1966; Narayanan and Rao, 1981, 1989) are: (i) strength decreases and base increases as one moves from the west to east AS, (ii) oscillation of its lateral boundary from west to east with the activity of monsoon and (iii) associated oscillation of mid tropospheric water vapor content from east to west, i.e. in the opposite sense to the boundary of temperature inversion. The two primary causes proposed (Colon, 1964) for formation/maintenance of monsoon inversion are: (a) hot air advection from Arabia (~ 700 hPa) riding over cool maritime air (at levels below ~ 800 hPa) from south Indian Ocean and (b) subsidence over western AS associated with monsoon convection over main land. This large scale subsidence had played a major role in the maintenance of MI during the prolonged weak monsoon of 2002 (Narayanan et al., 2004).

15 However, not much attention was paid to the study of MI due to paucity of freely available data over this region. The spatial density of TIROS-N satellite data available to the global, research community in 1979 was just a single temperature–humidity profile a day in a latitude–longitude grid box of $2.5^\circ \times 2.5^\circ$ (Kidder et al., 1995). Narayanan and Rao (1981) had to adopt temporally a pentad and spatially a $5^\circ \times 5^\circ$ average to detect statistically significant results from the meager data available then. Since 2008, the density of temperature and humidity profiles from polar orbiting satellites is nearly two orders of magnitude higher (about one vertical profile every $50 \text{ km} \times 50 \text{ km}$, twice each day and from two satellites) besides with a much better vertical and spectral resolution. Thus, it has become possible now to study MI phenomena in greater detail. However, no in-situ data after the 1979 experiment are available in this region.

25 In the present study, we have used the high resolution and better accuracy temperature and humidity profiles data obtained from Infrared Atmospheric Sounding Interferometer (IASI) onboard MetOp satellite. These data have higher vertical resolution, i.e., ~ 400 m below 700 hPa, which is much better than those of TIROS-N of MONEX

2.1 IASI observations

The IASI instrument (Clerbaux et al., 2007, 2009) measures the profiles of temperature profiles in the troposphere and lower stratosphere with a high accuracy (~ 1 K root mean square) at a vertical resolution of 1 km in the lower troposphere, as well as humidity profiles in the troposphere (10–15% accuracy with a 1–2 km vertical resolution) primarily for numerical weather prediction (Schlüssel et al., 2005). IASI is a thermal infrared nadir-looking Fourier transform spectrometer which measures the Earth's surface and the atmospheric radiation over a spectral range of 645–2760 cm^{-1} with a 0.5 cm^{-1} spectral resolution. The IASI field of view is a matrix of $2^\circ \times 2^\circ$ circular pixels, each with a diameter footprint of 12 km at nadir. It measures on an average at each location on the Earth's surface twice a day (at 09:30 and 21:30 h local time), every 50 km at nadir, with an excellent horizontal coverage due to its polar orbit and its capability to scan across track over a swath width of 2200 km. More details about retrieval and validation are presented in Kwon et al. (2012). The support products, which we have used, are available at 100 pressure levels at 50 km \times 50 km horizontal grid spacing.

2.2 Dropsonde/radiosonde measurements MONEX (1979)

For the in-situ ground truth comparisons over AS between the longitudes 55–75° E we also make use of the aircraft dropsondes and ship radiosonde observations obtained during MONEX 1979. MONEX was conducted during May–July 1979 and there were 416 radiosondes and 412 dropsondes measurements over AS. It may be noted that after the MONEX campaign in 1979, no campaign has been organized to get in-situ data over western or central AS. During the Indian ARMEX programme (2002), however, some in-situ data were available but only in the far eastern AS (east of 70°) near the coast of India. Table 2 summarizes the comparison of in-situ observations with satellite data of 1979 by Narayanan and Rao (1981). This information on ΔT criterion has been used as the basis in the present study.

2.3 ERA-Interim data

The European Centre for Medium Range Weather Forecasts (ECMWF)-Interim is one of most advanced in operational use for diagnosing the global atmosphere with an accuracy that is less than what is theoretically possible (Simmons and Hollingsworth, 2002; Simmons et al., 2007). The selected variables are specific humidity along with the temperature on different pressure levels. The atmospheric data are available at $0.125^\circ \times 0.125^\circ$ latitude and longitude grids on 37 pressure levels from 1000 to 1 hPa; however, we have used data of 14 pressure levels from 1000 to 600 hPa for the period of 2009 to 2013 for the present study. Vertical as well as horizontal strength of MI have been examined from these data sets and compared with satellite observations.

2.4 AIRS observations

AIRS onboard the Earth Observing System (EOS)-Aqua satellite of NASA was launched in 2002. This is also a polar orbiting satellite which crosses the equatorial latitudes at 13:30 and 01:30 h LT for the ascending and descending pass, respectively. The orbit period is 98.99 min, and the orbit is sun synchronous with consecutive orbits separated by 2760 km at the equator. AIRS has a field of view of 1.1° and provides a nominal spatial resolution of 13.5 km for IR channels and approximately 2.3 km for visible/near-IR channels. AIRS data together with data from the Advanced Microwave Sounder Unit (AMSU) (Lambrigtsen, 2003) are used in the present study. We make use of AIRS support data which have higher vertical resolution with 100 levels between 1100 and 0.016 hPa. For the present study we restrict data only from surface to 600 hPa which have vertical resolution of 30–20 hPa. Though these data are available since 2003, we make use data from 2009 only so as to compare with other data sets.

Characteristics of Monsoon inversions over Arabian Sea

Sanjeev Dwivedi et al.

Title Page

Abstract

Introduction

Conclusions

References

Tables

Figures



Back

Close

Full Screen / Esc

Printer-friendly Version

Interactive Discussion



2.5 COSMIC GPS RO

GPS RO technique is also a remote sounding satellite technique, and it uses the radio signals received onboard a low Earth orbiting satellite from atmospheric limb sounding. The GPS RO measurements have a vertical resolution ranging from 400 m to 1.4 km, which is much better than that of any other satellite data (Kursinski et al., 1997). COSMIC has vertical resolution of ~ 100 m in the lower troposphere for temperature. The COSMIC GPS RO was successfully launched in mid-April 2006 (Anthes et al., 2008). Since 17 July 2006, COSMIC GPS RO provides accurate and high vertical resolution profiles of atmospheric parameters that are almost uniformly distributed over the globe. COSMIC provides a direct estimate of refractivity (from measurement of bending angle by GPS technique) at very high vertical resolution, but have poor repetivity.

3 Methodology and analysis procedure

As mentioned earlier, MI was first observed by Colon (1964) and Ramage (1966) over the AS from ship upsonde profiles. They reported that MI lies between 900 and 800 hPa with strong intensity over western AS (WAS) and weakens as its base rises and comes to eastern AS (EAS). Following this study, Narayanan and Rao (1981) have shown MI's presence using the temperature difference (ΔT) between the TIROS-N derived sea skin temperature and atmospheric layer mean temperature (between 1000 and 850 hPa).

Note that lapse rate (dT/dz) of atmosphere at the tropospheric altitudes is a negative quantity. However, in this study (and also of Narayanan and Rao, 1981), we have considered ΔT as temperature difference between a lower level (higher temperature) and a higher level (lower temperature), so is normally a positive quantity of value $\sim +6$ to $+7$ K. For inversion regions, it is negative or a small positive quantity (i.e. less than $+2$ K).

After considering several limitations in the satellite data of that time, Narayanan and Rao (1981) finally considered MI when the difference ΔT , between surface and layer

Characteristics of Monsoon inversions over Arabian Sea

Sanjeev Dwivedi et al.

Title Page

Abstract

Introduction

Conclusions

References

Tables

Figures



Back

Close

Full Screen / Esc

Printer-friendly Version

Interactive Discussion



mean temperature (of 1000 to 850 hPa), is 2 K or less, which otherwise was greater than 3 K. Since then, several improvements in the satellite instruments, retrieval techniques and data products have come up in these three decades.

Extensive in-situ observations of AS MI features were obtained during FGGE-MONEX 1979 experiment. Figure 1a shows a typical example of MI observed in T (temperature) and RH (Relative Humidity) data obtained on 27 June 1979 at 06:56 GMT at 20° N, 62° E from radiosonde. In this example MI starts from surface and temperature departure is as high as ~ 10 K from a normal lapse rate profile at 900 hPa. The vertical extent of inversion varies from 0.5 km to even more than 1 km. It is to be noted that AS MI are much stronger and long lasting i.e. less diurnal variation than normal boundary layer and persist for many days compared to those over land regions.

A detailed analysis is made in this study by considering several thousands of profiles obtained from different satellite observations now available over AS for redefining MI. Since the MIs occur at low levels, first we tried with the earlier adopted criteria of Narayanan and Rao (1981) i.e., by taking difference between sea surface (skin) temperature and 925 hPa level (mean pressure level of 1000–850 hPa MLT of TIROS-N data of the 1980 time frame) temperature and found those to be noisy for detecting MI. To avoid the surface emissivity effects in the retrieval at/near surface (from the sounder instrument), we adopted the lower level in the present study as 950 hPa instead of sea surface/skin temperature. It was considered not appropriate to use SST/skin temperature (though may be of higher accuracy) from a different source (viz imager onboard the same satellite) for estimating ΔT . It was felt that this will not give the advantage of the differencing procedure employed earlier to detect inversion (Narayanan and Rao, 1981). This level criterion (950–850 hPa) was arrived at after a detailed examination of ΔT at a few more level intervals (viz 1000–900, 1000–850 hPa, etc).

Thus, we have used:

$$\Delta T = T(950 \text{ hPa}) - T(850 \text{ hPa}) \quad (1)$$

Characteristics of Monsoon inversions over Arabian Sea

Sanjeev Dwivedi et al.

Title Page

Abstract

Introduction

Conclusions

References

Tables

Figures



Back

Close

Full Screen / Esc

Printer-friendly Version

Interactive Discussion



Characteristics of Monsoon inversions over Arabian Sea

Sanjeev Dwivedi et al.

Title Page

Abstract

Introduction

Conclusions

References

Tables

Figures



Back

Close

Full Screen / Esc

Printer-friendly Version

Interactive Discussion



from a cursory examination of the data. The temperatures at a few/more levels were far wide of the normal profile. To account for these types of profiles, we applied a quality check to filter out spurious data. All profiles of July and August months of 2009 (poor monsoon year) and 2011 (normal monsoon year) were sorted out in $3^\circ \times 3^\circ$ boxes of WAS and EAS. For each month the mean and standard deviation were obtained for each interpolated levels separately. Those profiles for which the data at any one level was lying beyond ± 2 sigma of the mean, were not considered for further analysis. From this procedure we saw that nearly 25–30 % of profiles were getting filtered out.

Using these quality checked profiles, the procedure for selecting the right levels for calculating ΔT was established. Thereafter, for all the other monsoon days of the five years, we have computed ΔT for individual profiles by an automated procedure (without resorting to examining each profile). They were grouped and their ΔT values averaged in $1^\circ \times 1^\circ$ bins over the whole AS region. Diurnal variation of ΔT was examined for a few months of data. Once we made sure that this is not discernible, the day and night data of a calendar day were merged in $1^\circ \times 1^\circ$ boxes.

For further analysis, the average ΔT values for the day (24 h period) at $1^\circ \times 1^\circ$ grids have been used. Due to averaging of ΔT of all the profiles in $1^\circ \times 1^\circ$ box and morning and evening passes (~ 6 to 8 values of ΔT in 24 h), the strength of MI may be getting somewhat reduced (as MI occur at slightly different levels within a vertical range of 25–50 hPa, for different profiles in the same $1^\circ \times 1^\circ$ box). For some studies (e.g. for Figs. 2, 4 and 5, etc), we have used only a limited data from this total data set. The total number of profiles considered for the five years amount to nearly half a million, each for AIRS and IASI – considering that nearly 30 % profiles did not pass through our quality check.

4 Results and discussions

4.1 Monsoon inversions observed in satellite and ERA-Interim datasets

Figure 1a and b show MI observed on 27 June 1979 at 07:30 GMT at 20° N, 60° E through MONEX radiosonde and ERA-Interim data, respectively. The detailed comparison study between TIROS-N satellite data of 1979 and concurrent in-situ MONEX radiosonde profiles for 1979 southwest monsoon carried out by Narayanan and Rao (1981) is summarized in Table 2. This was the only occasion (1979) when in-situ data were available over AS to compare with satellite soundings. Thus, comparison of current satellite observations is being done in this study with ERA-Interim data. In this case, ERA-Interim data also catches the inversion but with a less rise in temperature (~ 3–4 K) and decrease in RH (~ 60 %). To show how the present day satellites reveal MI, typical profiles of temperature and RH obtained from collocated IASI and ERA-Interim on 30 July 2009, 05:30 GMT are plotted in Fig. 1c and d, respectively. A clear MI in the satellite profile and ERA-Interim can be noticed though with somewhat varying strengths. These are the first reported results of MI features seen directly from the satellite observations over the AS which were shown earlier by Narayanan and Rao (1981) in an indirect way by using ΔT indices. In general, in the individual satellite profiles, we are able to see the MI strengths ranging from ~ +2 to –6 K (–8.8 K being the actual temperature difference between 930 and 850 hPa in Fig. 1c). These MI lie mostly below 850 hPa level, but in rare occasions we could see them even up to 700 hPa over the EAS – but of much weaker strength. The strength of MI is also seen to be decreasing from WAS to EAS which will be discussed in detail in later sections.

Thus, in Fig. 1, we have seen examples of MI comparison between radiosonde and ERA interim (1979) and between IASI and ERA-Interim (2009). There are some minor inconsistencies by way of inversion heights in individual profiles of the three data sets. However, our objective here is to examine the large scale characteristics of MI by considering average ΔT computed from individual profiles in $1^\circ \times 1^\circ$ grids.

Title Page

Abstract

Introduction

Conclusions

References

Tables

Figures



Back

Close

Full Screen / Esc

Printer-friendly Version

Interactive Discussion



4.2 Contrasting behavior of MI between WAS and EAS

As observed from Fig. 1, MI can lie between surface and ~ 2 km during Indian Summer Monsoon (ISM) season (JJAS). Careful examination of time evolution of ΔT over the western Arabian sea reveals that the MI start forming around first half of May and dissipate around late September. Figure 2 shows the evolution of the MI during two contrasting years (2009 a poor monsoon year and 2011 a normal monsoon year). During the peak monsoon season of July–August, the difference in ΔT between the two years are prominently noticed. Also MI is more frequently observed with higher strength during the peak monsoon months of July and August. To investigate further their contrasting features in WAS and EAS, data only of July and August from 2009 to 2013 are presented.

In Fig. 3 we have summarized the three important characteristics of MI viz their base altitude, strength (as revealed by ΔT) and percentage occurrence during the complete season. For brevity, the results of only July and August months, averaged for all the five years 2009–2013 are shown in the figures. Figure 3a and b shows the spatial variation of base altitude of MI during July and August, respectively. The contrasting feature of base altitude of occurrence of MI is seen mainly north of 15° N from the selected three grid boxes. It increases from WAS (below 1 km) to EAS (above 1.5 km) through CAS (1.0–1.5 km).

As mentioned earlier, from very limited observations previous studies (Colon, 1964; Ramage, 1966; Narayanan and Rao, 2004) had suggested that strength and frequency of occurrence of the MI will be more over WAS than over EAS. To investigate this contrasting behavior of MI in detail from satellite soundings, we examined the spatial variations of ΔT . Figure 3c (July) and d (August) shows the strength of MI increasing from EAS to the WAS and is prevalent mainly north of 15° N latitude extending from 15 to 25° N latitude and 55 to 68° E longitude. The strength of MI can be noticed as $\sim +2$ K near Arabia coast and as we approach Indian coast, the normal environmental lapse rate condition of $+6$ to $+7$ K km $^{-1}$ are encountered. From these figures a clear

Characteristics of Monsoon inversions over Arabian Sea

Sanjeev Dwivedi et al.

Title Page

Abstract

Introduction

Conclusions

References

Tables

Figures



Back

Close

Full Screen / Esc

Printer-friendly Version

Interactive Discussion



Characteristics of Monsoon inversions over Arabian Sea

Sanjeev Dwivedi et al.

Title Page

Abstract

Introduction

Conclusions

References

Tables

Figures



Back

Close

Full Screen / Esc

Printer-friendly Version

Interactive Discussion



contrast in ΔT a difference of around 2 K in the southeast quadrant of AS between July and August is also noticed. In general, the AS is covered with lapse rate of $+4 \text{ K km}^{-1}$, which is the condition for taking the atmosphere towards stability during the August month. The region of Somali low level jet is the location of permanent region of MI during the month of July. Strong surface winds of south-west monsoon produce an Ekman transport perpendicular to the wind flow with strong upwelling in the region which in turn brings the cool water from the deeper layers to surface. Simon et al. (2007) showed that WAS region is the region of Somali upwelling, and also since the low level jet and surface wind are of the order of $\sim 20 \text{ m s}^{-1}$, they produce sufficient cooling and the air above this region is still warmer when compared to the upwelling area, producing strong inversion.

Figure 3e and f shows the spatial variation of percentage occurrence (PO) of MI during July and August months. PO is calculated corresponding to $\Delta T \leq +2 \text{ K}$ criteria. In general, it is observed that WAS show more number of MI cases (50 to 70 %) compared to EAS (10 to 20 %). ERA-Interim data show only 30 to 50 % cases of MI over WAS which will be dealt in detail in the following sub-sections. The maximum PO during the four months of monsoon over the WAS are 40 % (June), 60 % (July), 50 % (August) and 30 % (September) (figure not shown). The areal extent of the maximum PO is seen during July. During September, very small area of Northern AS is covered with $\sim 50 \%$. No inversion is seen in the EAS box during the June and September periods. Despite its low strength (ΔT) PO show maximum occurrence of 60 % in July. Since the PO and strength of MI over the CAS is in between the features of EAS and WAS, for further discussions pertain, only WAS and EAS boxes.

The PO of ΔT value in different ranges observed in IASI for the five monsoon seasons is shown in Fig. 4. ΔT values range from -2 to $+6 \text{ K}$ (0 to $+7 \text{ K}$) in WAS (EAS) with peak occurring around $+1$ to $+2 \text{ K}$ ($+3$ to $+4 \text{ K}$). There are only a few values of ΔT less than $+2 \text{ K}$ in EAS. Similar analysis is also made using ERA-Interim data and is shown in bottom panels of Fig. 4. ERA-Interim data shows the contrast between WAS and EAS more clearly. In case of q at 700 hPa a difference of about 2 g kg^{-1} can be no-

ticed, with EAS having higher humidity values than WAS in IASI. However, ERA-Interim data does not show this distinction.

To further examine the contrasting behavior between EAS and WAS, time series of ΔT and water vapour at 700 hPa is considered for different years. Daily mean variations of ΔT and specific humidity, q , at 700 hPa in WAS and EAS during the monsoon season of the year 2012 observed by IASI is shown in Fig. 5. Note that we have included results of all the days irrespective of whether MI is present or not. Three point average smoothed curves are shown in the respective panels. In general, it can be seen that WAS ΔT (q at 700 hPa) values are $\sim +2$ K ($1-2$ gkg $^{-1}$) less than those over EAS for the season as a whole (Fig. 5a and b). During all the years (2009–2013) of the present study, IASI reveals (figure not shown) this feature. Similar analysis has been carried out using ERA-Interim reanalysis data and is shown in Fig. 5c and d. A clear contrast between WAS and EAS in ΔT can be noticed in ERA-Interim data. A mean difference of ~ 2 K (~ 1 gkg $^{-1}$) can be noticed in ΔT (q at 700 hPa) between WAS and EAS, EAS values being lower. A cyclic behavior in ΔT variations with a period of $\sim 20-25$ days in case of ERA-Interim is noticed but not observed in the satellite measurements. There exists no significant diurnal variation in ΔT (figure not shown). This was verified before averaging ΔT of all profiles (day and night) in the $1^\circ \times 1^\circ$ grids. Due to inversion and stability, moisture is getting trapped at lower levels over WAS compared to EAS as indicated in Fig. 5b and d observed from IASI and ERA-Interim, respectively.

4.3 Relation between MI over AS and monsoon activity

Past investigations (e.g. Gadgil and Joseph, 2003) showed that the mesoscale monsoon features largely vary with the activity of the monsoon. In general during the active phase of the ISM, typically there will be more precipitation over central India ($18-28^\circ$ N and 65° to 88° E). Similar variations in precipitation during the monsoon season can also be expected on regional scales. Gadgil and Joseph (2003), Kripalani et al. (2004), Rajeevan et al. (2006) have considered the daily rainfall time series over central India during monsoon months along with the climate normal to delineate “active” and “break”

Characteristics of Monsoon inversions over Arabian Sea

Sanjeev Dwivedi et al.

Title Page

Abstract

Introduction

Conclusions

References

Tables

Figures



Back

Close

Full Screen / Esc

Printer-friendly Version

Interactive Discussion



as blue line in Fig. 9c. We can infer that if ΔN is less than 50 N units it corresponds to non-inversion region (ΔN more than 50 may be inversion or otherwise). ΔN is thus a supportive parameter to ΔT in identifying inversion/non inversion. Because of its larger dynamic range, details of inversion have been identified in the ΔT and ΔN maps (figure not shown).

It is well known that COSMIC satellites are able to provide N profiles directly. The spatial and temporal sampling of COSMIC at any particular region are, however, very meagre. The comparison map of ΔN from IASI and ΔN from COMIC combined for a long break spell from 30 July to 11 August 2009 has been studied. This long period accumulation of data was necessary to have sufficient data points from COSMIC to cover the entire AS. One can see ΔN values above 50 N units (inversion region) covering the entire Arabian sea corresponding to ΔT values being below 2 K (shown by IASI, figure not shown). Over the AS region ΔN observed for all the five years of our study was combined to produce the frequency distribution of ΔN over Western AS (5–25° N, 56–65° E, excluding land) and Eastern AS (5–25° N, 66–75° E, excluding land) and is shown in Fig. 10. Over WAS, 712 cases and over EAS 547 cases are showing $\Delta N > 50N$ units (which may be supportive to inversion). A difference of about 10N units can be noticed, with WAS having higher ΔN values.

5 Summary and conclusions

Low level MI characteristics, which usually occur below 700 hPa over the AS during southwest monsoon months, have been identified directly from operational satellite temperature retrievals. For the first time we have shown here cases of direct and unambiguous delineation of MI from the satellite temperature and water vapor retrieval observations. We have used five years (2009–2013) data of two different satellite sounder instruments (mainly from IASI and for inter comparison AIRS) along with ERA-Interim reanalysis data to delineate the characteristics of MI over AS. Their percentage occurrence, base height and strength have been studied. For supporting our findings, we

Characteristics of Monsoon inversions over Arabian Sea

Sanjeev Dwivedi et al.

Title Page

Abstract

Introduction

Conclusions

References

Tables

Figures



Back

Close

Full Screen / Esc

Printer-friendly Version

Interactive Discussion



also compare with the campaign of MONEX 1979 in-situ measurements over AS. The main findings obtained from the observational study are summarized in the following:

1. Percentage occurrences of MI over WAS (up to $\sim 65^\circ$ E) is ~ 60 – 70% and are always higher and stronger than over EAS. WAS ΔT values are ~ 2 K less than those over EAS.
2. MI is stronger during poor monsoon year (2009) and occurs on more occasions in WAS during break spells. Whether this is true or not for all poor monsoon years need to be checked with more years of data.
3. ERA-Interim is also able to provide these features but is restricted to some parts of AS with more smoothed variability.
4. Inter-comparison of IASI and AIRS profiles from the view of study of inversion suggests the differences do not warrant a mix of these two data sets for this study.
5. The refractivity data has only a supporting role to identify monsoon inversion regions.

Thus, MI seems to be a semi-permanent feature of Indian summer monsoon. It is suggested to include this feature also in future monsoon diagnostic and forecast studies.

Acknowledgements. This work is a part of the INSAT-3-D project sponsored by the Indian Space Research Organization (ISRO), for which we are thankful to Space Applications Centre, Ahmadabad. We wish to thank C. M. Kishtawal, V. Sathiyamoorthy, S. GhouseBasha, Jyotirmayee and Ranjit Thapa for discussions and for help in data processing aspects and help in using HPCC. The authors would like to thank ECMWF (<http://apps.ecmwf.int/datasets>) for providing data of ERA-Interim, GESDISC (<http://mirador.gsfc.nasa.gov/forAIRS>) for AIRS, NOAA (<http://www.nsof.class.noaa.gov/forIASI>) for IASI through ftp. We also thank IMD for providing rainfall data over Indian land mass.

Characteristics of Monsoon inversions over Arabian Sea

Sanjeev Dwivedi et al.

Title Page

Abstract

Introduction

Conclusions

References

Tables

Figures



Back

Close

Full Screen / Esc

Printer-friendly Version

Interactive Discussion



References

- Anthes, R. A., Bernhardt, P. A., Chen, Y., Cucurull, L., Dymond, K. F., Ector, D., Healy, S. B., Ho, S. P., Hunt, D. C., and Kuo, Y. H.: The COSMIC/FORMOSAT-3 mission: early results, *B. Am. Meteorol. Soc.*, 89, 313–333, doi:10.1175/Rep.BAMS-89-3-313, 2008.
- 5 Basha, G. and Ratnam, M. V.: Identification of atmospheric boundary layer height over a tropical station using high-resolution radiosonde refractivity profiles: comparison with GPS radio occultation measurements, *J. Geophys. Res.*, 114, D16101, doi:10.1029/2008JD011692, 2009.
- Bhat, G. S.: The Indian drought of 2002: a sub-seasonal phenomenon, *Q. J. Roy. Meteor. Soc.*, 10 32, 2583–2602, 2006.
- Clerbaux, C., Hadji-Lazaro, J., Turquety, S., George, M., Coheur, P. F., Hurtmans, D., Wespes, C., Herbin, H., Blumstein, D., and Tourniers, B.: The IASI/MetOp mission: first observations and highlights of its potential contribution to GMES, *COSPAR Inf. Bul.*, 168, 19–24, 2007.
- Clerbaux, C., Boynard, A., Clarisse, L., George, M., Hadji-Lazaro, J., Herbin, H., Hurtmans, D., 15 Pommier, M., Razavi, A., Turquety, S., Wespes, C., and Coheur, P.-F.: Monitoring of atmospheric composition using the thermal infrared IASI/MetOp sounder, *Atmos. Chem. Phys.*, 9, 6041–6054, doi:10.5194/acp-9-6041-2009, 2009.
- Colon, J. A.: On interactions between the Southwest Monsoon current and the sea surface over the Arabian Sea, *Indian J. Meteor. Geophys.*, 15, 183–200, 1964.
- 20 Das, P. K.: *The Monsoons*, Nation Book Trust, New Delhi, India, ISBN 978-81-237-1123-2, 193, 2002.
- Gadgil, S. and Joseph, P. V.: On breaks of the Indian monsoon, *Proc. Indian Acad. Sci.*, 112, 529–558, 2003.
- Kidder, S. Q. and Haar, T. H. V.: *Satellite Meteorology – An Introduction*, Academic Press Inc., 25 California, USA, ISBN 0-12-406430-2, 1995.
- Kripalani, R. H., Kulkarni, S. A., Sabade, S., Revadekar, J. V., Patwardhan, S. K., and Kulkarni, J. R.: Intra-seasonal oscillations during monsoon 2002 and 2003, *Curr. Sci. India*, 87, 325–331, 2004.
- 30 Kwon, E. H., Sohn, B. J., William, L., and Smith, J. L.: Validating IASI temperature and moisture sounding retrievals over East Asia using radiosonde observations, *J. Atmos. Ocean. Tech.*, 29, 1250–1262, doi:10.1175/JTECH-D-11-00078.1, 2012.

Characteristics of Monsoon inversions over Arabian Sea

Sanjeev Dwivedi et al.

Title Page

Abstract

Introduction

Conclusions

References

Tables

Figures



Back

Close

Full Screen / Esc

Printer-friendly Version

Interactive Discussion



Characteristics of Monsoon inversions over Arabian Sea

Sanjeev Dwivedi et al.

Title Page

Abstract

Introduction

Conclusions

References

Tables

Figures



Back

Close

Full Screen / Esc

Printer-friendly Version

Interactive Discussion



Kursinski, E. R., Hajj, G. A., Schofield, J. T., Linfield, R. P., and Hardy, K. R.: Observing Earth's atmosphere with radio occultation measurements using the Global Positioning System, *J. Geophys. Res.*, 102, 23429–23466, doi:10.1029/97JD01569, 1997.

Lambrigtsen, B. H.: Calibration of the AIRS microwave instruments, *IEEE T. Geosci. Remote*, 41, 369–378, 2003.

Narayanan, M. S. and Rao, B. M.: Detection of monsoon inversion by TIROS-N satellite, *Nature*, 294, 546–548, 1981.

Narayanan, M. S. and Rao, B. M.: Stratification and convection over Arabian Sea during monsoon 1979 from satellite data, *Proc. Indian Acad. Sci.*, 98, 4, 339–352, 1989.

Narayanan, M. S., Rao, B. M., Shah, S., Prasad, V. S., and Bhat, G. S.: Role of atmospheric stability over the Arabian Sea and the unprecedented failure of monsoon 2002, *Curr. Sci. India*, 86, 7, 938–947, 2004.

Rajeevan, M. and Bhate, J.: A high resolution daily gridded rainfall data set (1971–2005) for mesoscale meteorological studies, *Curr. Sci. India*, 96, 558–562, 2009.

Rajeevan, M., Bhate, J., Kale, J. D., and Lal, B.: High resolution daily gridded rainfall data for the Indian region: analysis of break and active monsoon spells, *Curr. Sci. India*, 91, 296–306, 2006.

Ramage, C. S.: The summer atmospheric circulation over the Arabian Sea, *J. Atmos. Sci.*, 23, 144–150, 1966.

Sathiyamoorthy, V., Mahesh, C., Gopalan, K., Prakash, S., Shukla, B. P., and Mathur, A. K.: Characteristics of low clouds over the Arabian Sea, *J. Geophys. Res.*, 118, 13489–13503, 2013.

Schlüssel, P., Hultberg, T. H., Philipps, P. L., August, T., and Calbet, X.: The operational IASI level 2 processor, *Adv. Space Res.*, 36, 982–988, doi:10.1016/j.asr.2005.03.008, 2005.

Simmons, A. J. and Hollingsworth, A.: Some aspects of the improvement in skill of numerical prediction, *Q. J. Roy. Meteor. Soc.*, 128, 647–677, 2002.

Simmons, A., Uppala, S., Dee, D., and Kobayashi, S.: ERA-Interim: New ECMWF reanalysis products from 1989 onwards, *Newsletter 110 – Winter 2006/07*, ECMWF, 11 pp., 2007.

Simon, B., Rahman, S. H., Joshi, P. C., and Desai, P. S.: Shifting of the convective heat source over the Indian Ocean region in relation to performance of monsoon: a satellite perspective, *Int. J. Remote Sens.*, 29, 387–397, doi:10.1080/01431160701271966, 2007.

Smith, N., Smith Sr., W. L., Weisz, E., and Revercomb, H. E.: AIRS, IASI, and CrIS retrieval records at climate scales: an investigation into the propagation of systematic uncertainty, *Am. Meteor. Soc.*, 54, 1565–1481, doi:10.1175/JAMC-D-14-0299.1, 2015.

5 Susskind, J., Barnet, C. D., and Blaisdell, J. M.: Retrieval of atmospheric and surface parameters from AIRS/AMSU/HSB data in the presence of clouds, *IEEE Trans. Geosci. Remot Sens.*, 41, 390–409, 2003.

Thomas, W. S.: An assessment of operational TIROS-N temperature retrievals over the United States, *Mon. Weather Rev.*, 109, 110–119, 1981.

10 Wallace, J. M. and Hobbs, P. V., *International Geophysics series: Atmospheric Science – an Introductory Survey*, 2nd edn., 92, California, USA, Academic Press, ISBN 13:978-0-12-732951-2, 391, 2006.

WMO: GARP Publication series no. 18, *The Monsoon Experiment*, Geneva, Switzerland, 1976.

Characteristics of Monsoon inversions over Arabian Sea

Sanjeev Dwivedi et al.

Title Page

Abstract

Introduction

Conclusions

References

Tables

Figures



Back

Close

Full Screen / Esc

Printer-friendly Version

Interactive Discussion



Characteristics of Monsoon inversions over Arabian Sea

Sanjeev Dwivedi et al.

Table 1. Data details for accuracy/error and availability.

	IASI	AIRS	COSMIC GPS – RO	ERA-Interim	MONEX 1979 In-situ data
Launch of satellite	MetOp – a launched in Oct 2006, 8461 spectral Channels Aug 2008	Aqua launched in May 2002, 2378 spectral channels 2003	GPS – RO microsatellite receiver launched in Apr 2006	–	May–Aug 1979
Data availability from	Jun–Sep 2009–2013	Jun–Sep 2009–2013	Jun–Sep 2009–2013	1979	May–Aug 1979
Data used in the present study	Jun–Sep 2009–2013	Jun–Sep 2009–2013	Jun–Sep 2009–2013	Jun–Sep 2009–2013	May–Aug 1979
Accuracy in Temperature	~ 1 K(RMS) at a vertical resolution of 1 km (Clerbaux et al., 2007, 2009)	~ 1 K at a vertical resolution of 1 km (Susskind et al., 2003)	Generally ~ 100 m in the lower troposphere (not for T)	0.5–1.0 K at a vertical resolution of 0.8–1.0 km	±1 °C in 4 vertical levels resolution (WMO report)
Accuracy in Humidity	~ 10–15 % accuracy with a 1–2 km vertical resolution (Clerbaux et al., 2007, 2009) (Schlüssel et al., 2005)	~ 15 % accuracy with a 2 km vertical layer resolution (Susskind et al., 2003)	–	~ 7.0–20 % at a vertical resolution of 0.8–1.0 km	±30 % at a vertical resolution of 4 levels.
Accuracy in Refractivity	–	–	400 m to 1.4 km (Kursinski et al., 1997), 2000 soundings per day	1.5° × 1.5° (~ 80 km)	500 km
Horizontal resolution	15 km	25 km	70 % of occultations penetrate below 1 km (Anthes et al., 2008)	1013–1 hPa 37	1000–294
Pressure levels	1100–0.0161 hPa –100	1100–0.0161 hPa –100	–	–	Different –2
Local equator crossing time Swath	09:30 LT descending node 2200 km	13:30 LT ascending node 1650 km	–	–	–

Title Page

Abstract

Introduction

Conclusions

References

Tables

Figures



Back

Close

Full Screen / Esc

Printer-friendly Version

Interactive Discussion



Characteristics of Monsoon inversions over Arabian Sea

Sanjeev Dwivedi et al.

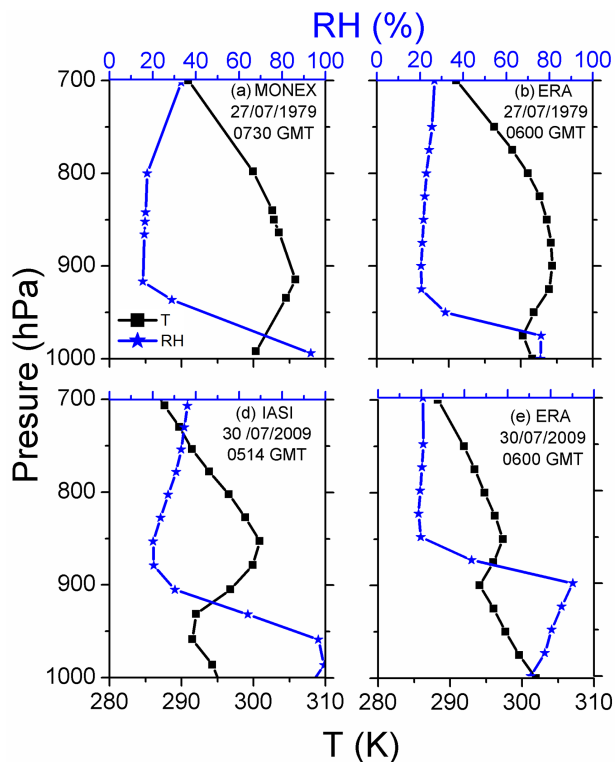


Figure 1. Typical examples showing MI in T and RH on **(a)** 27 June 1979 at 07:30 GMT at 20° N, 60° E obtained from radiosonde from MONEX experiment, **(b)** same as **(a)** but at 06:00 GMT from ERA, **(c)** 30 July 2009 at 05:14 GMT at 22° N, 68° E by IASI, **(d)** 30 July 2009 by ERA-Interim at same location but at 06:00 GMT. Note that scale for RH is shown in the top axis of **(a)** and **(b)**.

[Title Page](#)
[Abstract](#)
[Introduction](#)
[Conclusions](#)
[References](#)
[Tables](#)
[Figures](#)
[◀](#)
[▶](#)
[◀](#)
[▶](#)
[Back](#)
[Close](#)
[Full Screen / Esc](#)
[Printer-friendly Version](#)
[Interactive Discussion](#)


Characteristics of Monsoon inversions over Arabian Sea

Sanjeev Dwivedi et al.

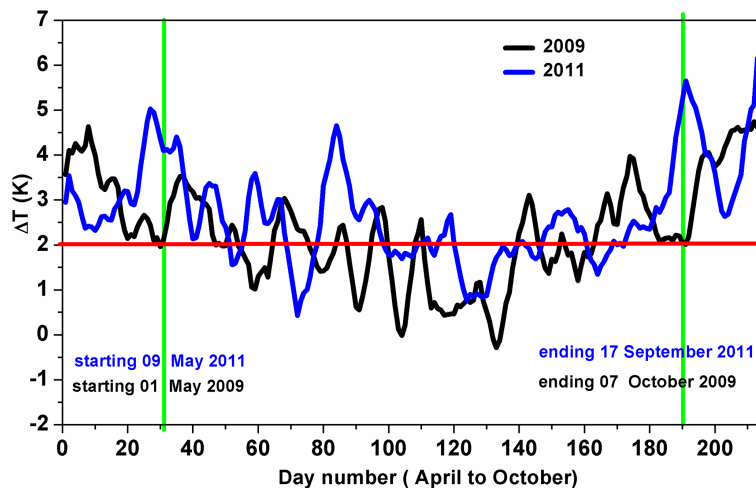


Figure 2. Time series of ΔT for starting and ending of MI from April to October 2009 (black) and 2011 (blue). Green vertical lines are showing starting (1 May 2009) and ending (7 October 2009) time for MI.

[Title Page](#)[Abstract](#)[Introduction](#)[Conclusions](#)[References](#)[Tables](#)[Figures](#)[Back](#)[Close](#)[Full Screen / Esc](#)[Printer-friendly Version](#)[Interactive Discussion](#)

Characteristics of Monsoon inversions over Arabian Sea

Sanjeev Dwivedi et al.

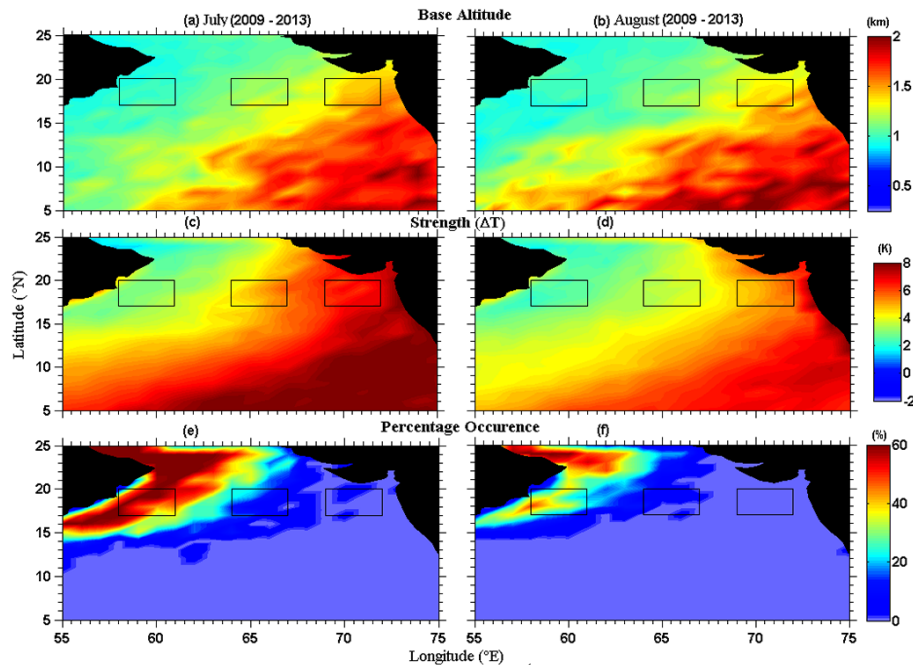


Figure 3. Base altitude occurrence of MI during **(a)** July, **(b)** August, ΔT (Strength) of MI **(c)** July, **(d)** August, and Percentage occurrence of MI **(e)** July, **(f)** August, averaged during 2009–2013 observed by IASI. (We are selecting WAS, CAS and EAS from this figure.)

[Title Page](#)
[Abstract](#)
[Introduction](#)
[Conclusions](#)
[References](#)
[Tables](#)
[Figures](#)
[◀](#)
[▶](#)
[◀](#)
[▶](#)
[Back](#)
[Close](#)
[Full Screen / Esc](#)
[Printer-friendly Version](#)
[Interactive Discussion](#)


Characteristics of Monsoon inversions over Arabian Sea

Sanjeev Dwivedi et al.

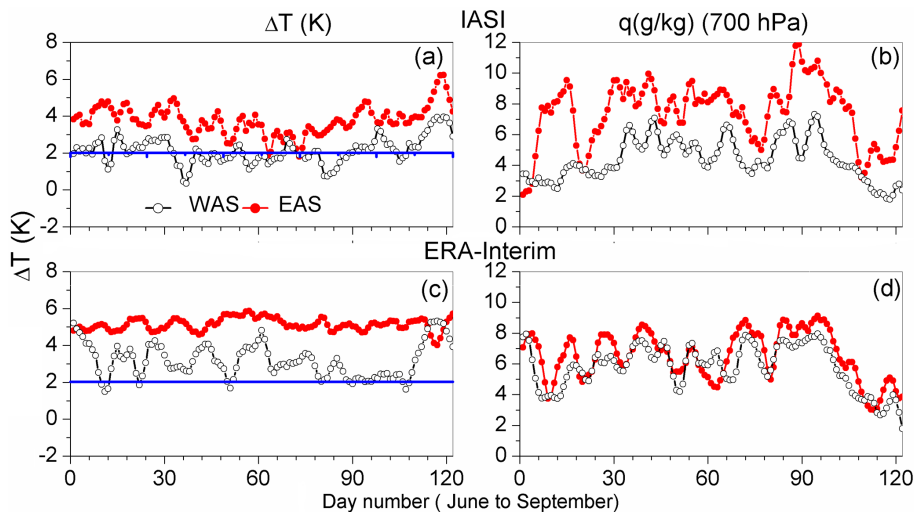


Figure 5. Time series of (a) ΔT and (b) q at 700 hPa observed over WAS and EAS grid boxes during the monsoon season of the year 2012 by IASI, (c) and (d) same as (a) and (b) but obtained using ERA-Interim data. 3-point smoothed curves are shown.

Characteristics of Monsoon inversions over Arabian Sea

Sanjeev Dwivedi et al.

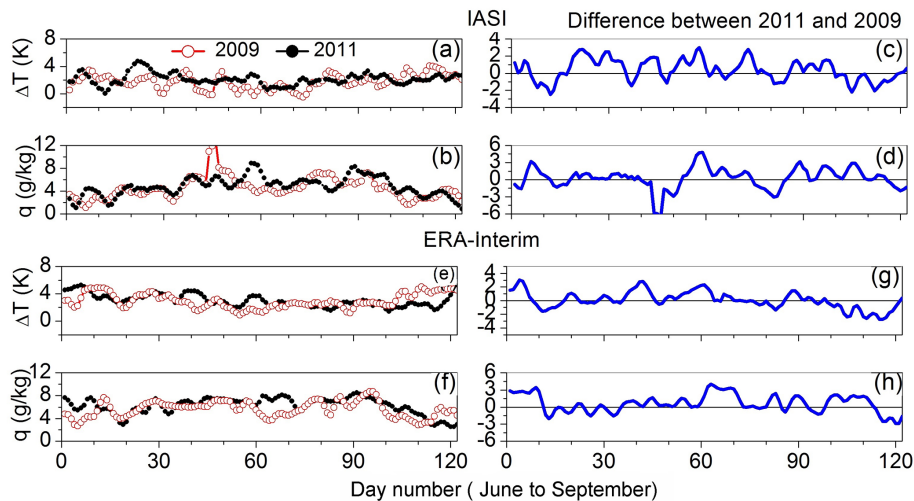


Figure 7. Time variations of (a) ΔT and (b) q at 700 hPa observed over WAS during two contrasting years of 2009 and 2011 by using IASI measurements. Difference between 2011 and 2009 observed in (c) ΔT and (d) q at 700 hPa. (e) to (h) same as (a) to (d) but observed by using ERA-Interim data.

Title Page

Abstract

Introduction

Conclusions

References

Tables

Figures



Back

Close

Full Screen / Esc

Printer-friendly Version

Interactive Discussion



Characteristics of Monsoon inversions over Arabian Sea

Sanjeev Dwivedi et al.

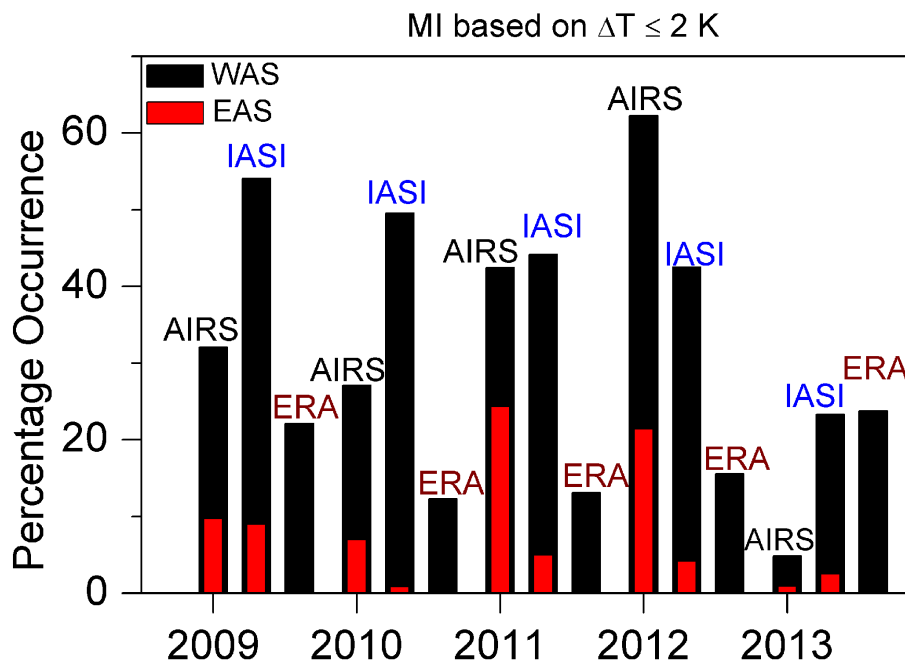


Figure 8. Percentage occurrence of MI observed with (a) $\Delta T \leq 2$ K using IASI, AIRS and ERA-Interim data during monsoon seasons of 2009–2013 over WAS and EAS.

Title Page

Abstract

Introduction

Conclusions

References

Tables

Figures



Back

Close

Full Screen / Esc

Printer-friendly Version

Interactive Discussion



